Performance Analysis of Bi-Orthogonality based Systems for 5G Internet of Machine Critical Things Communications

Ravi Sekhar Yarrabothu[1], Usha Rani Nelakuditi[2]

Department of ECE
Vignan's Foundation for Science, Technology and Research, Vadlamudi, India.
Email [1]: ykravi@gmail.com; Email [2]:usharani.nsai@gmail.com

***Abstract* - The vast set of connections among devices via the Internet is well-known as the Internet of Things (IoT). The mandate for 5G cellular communication is to support the IoT and Internet of Machine Critical Things (IoMCT) communications along with traditional voice, video and data communications. The IoMCT plays a crucial role in machine critical tasks such as battlefields, disaster management, and infrastructure surveillance. IoMCT applications demands ultra low cost and low power solutions. In order to cater the needs of IoMCT services, innovative physical layer solutions are need to be developed based on the existing Long Term Evolution (LTE) 4G cellular systems. One such solution is to design a new waveform for the 5G cellular communication systems which can handle a diversified requirements and varied traffic types. In this paper, a new access method within the ambit of 3GPP defined LTE procedures is discussed to support IoMCT generated sporadic traffic. The main problem to be addressed is handling of simultaneous transmission of data and control traffic. A new waveform based on bi-orthogonal frequency division multiplexing with Offset Quadrature Amplitude Modulation (OQAM) is proposed in this paper. BFDM system with QAM and OQAM are simulated using Matlab Software and the simulation results shows that the proposed the OQAM based BFDM waveform approach is better compared to the conventional random access using OFDM under various real time fading conditions defined by 3GPP for LTE.**

Keywords - OFDM, OQAM, BFDM, 5G, IoT, MTC, IoMCT, LTE, 3GPP

I. INTRODUCTION

The next turf of war for telecom operators is to provide ultra high bandwidth to mobile users with the real time information at anytime and anywhere. The key drivers of 5G Research are Internet of Things (IoT), Gigabit Connectivity everywhere, Tactile Internet. The Internet of Things (IoT) is going to be one of the key drivers for the growth of 5G networks[1] and sporadic traffic generating devices need to be provided the efficient access to networks. IoMCT devices will be inactive for larger time periods and the internet is accessed periodically for minor or incremental update without human intervention. The drastic increase of sporadic traffic in the 5G networks cannot be handled with the bulky LTE random access procedures.

In this paper as proposed in [2], [3], a new approach is used to efficiently handle sporadic traffic of 5G by using an enhanced physical layer random access channel (PRACH), which achieves device acquisition and transmission of small data payloads simultaneously. By doing so, without maintaining a continuous connection, PRACH is used to transmit smaller data packets like in UMTS. In LTE the user data is carried only by using the physical uplink shared channel (PUSCH) and due to this scalable sporadic traffic is not possible. In 3GPP Release 13, the physical layer enhancements [4] are introduced for enhanced machine-type communications (eMTC). 5G Now [2] proposed a design of arranging a data access section in between the synchronization PUSCH and normal PRACH, which is called as Data PRACH (D-PRACH) to support transmission of asynchronous data. The guard band between PRACH and PUSCH is used by D-PRACH and in this way the sporadic traffic is removed from the uplink data channel PUSCH, which results in to a very significant reduction in signaling overhead and reduction in power consumption of the devices. Sacrificing the guard bands for data transmission, normally leads to augmented interference for PUSCH users, which can be taken care by newer waveform designs.

In Bi-Orthogonal Frequency Division Multiplexing (BFDM), normal orthogonality is replaced with a set of pair wise orthogonal transmit and receives pulses. Consequently, more flexibility is obtained for the design of transmit prototypes with suppression of side lobes. Matched filter is not suitable for BFDM and in this paper a mismatched ZF filter is used[5]. The PRACH symbol transmission is very much immune to time offsets due to the long symbol duration and so the BFDM design is well suited for transmission of sporadic traffic. BFDM shows exceptional and controllable performance degradation trade-off between the time and frequency offsets in comparison with conventional OFDM. BFDM with OQAM shows superior robustness to delay/doppler spread and additive noise when compared with OFDM/QAM systems

This paper is organized is in four sections. The section II, describes the design of BFDM system, Section III talks about the OQAM based BFDM, Section IV discuses the system setup and simulation and simulation results are presented in section IV. Finally conclusions and future work is mentioned in section VI.

II. BFDM SYSTEM DESIGN

Pulse shaping method is used by Bi-orthogonal frequency division multiplexing (BFDM) for PRACH transmissions. Similar to OFDM, the symbols are transmitted as per a group of pulses shifted on time-frequency lattice points (kT,lF),where T is time shift and F is the Frequency shift period and $k,l\in\mathbb{Z}$. As mentioned in [2], the exact reconstruction of symbol is possible only if bi-orthogonal Riesz bases is formed by transmit pulses $\{g_{k;l}\}$ and the receive pulses $\{\gamma_{k;l}\}$. Two factors namely pulse properties and the time-frequency product TF (>1) will determine the possibility of perfect symbol reconstruction. In this paper we chose the TF=1.25.

A. Transmitter

in LTE, where Zadoff-Chu sequences are used for PRACH, BFDM transmitter uses a single-tone PRACH transmission [4].

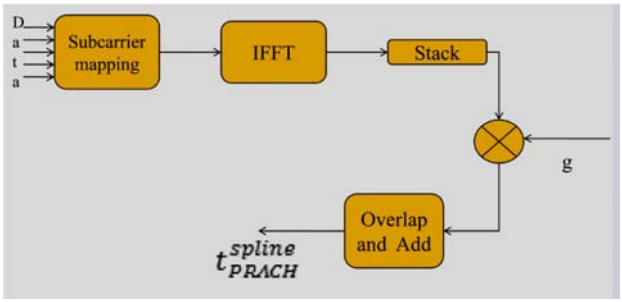

Figure 1 BFDM PRACH transmitter

Shaping of the PRACH signal spectrum is done by using a pulse g. Let 'P' be the length of pulse g. The transmitted signal t[n] generated after the inverse FFT (IFFT) stage by iterating and taking modulo P, which is of same length P. Given k symbols, each symbol t_k [n]is stacked as row matrix

$$T=\begin{pmatrix} t_0[n] \\ t_1[n] \\ \vdots \\ t_{K-1[n]} \end{pmatrix},\text{S}\in \mathbb{C}^{KxP} \quad (1)$$

Each t_k [n]is point wise multiplied with the shifted pulse g and superimposed by overlap and add. Then, the base band pulse shaped PRACH transmit signal is

$$t_{pr}^{ps}[n]=\sum_{k=0}^{K-1} t_k\,[n]g[n-kN] \quad (2)$$

B. Receiver

Pulse shaped PRACH receiver is a shown in the figure 2. First an inversion operation is carried out on the transmitter side pulse. Here the first K symbols of the received signal $o_{PR}[n]$ are arranged in a row vector matrix

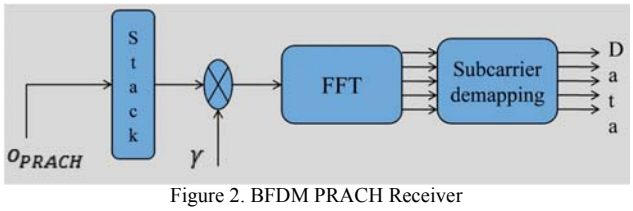

Figure 2. BFDM PRACH Receiver

$$\text{O}=\begin{pmatrix} o_0[n] \\ o_1[n] \\ \vdots \\ o[n] \end{pmatrix},\text{R}\in \mathbb{C}^{KxP} \quad (3)$$

Then each row is multiplied point wise by the shifted bi-orthogonal pulse γ , so the received signal is

$$o_k^{\gamma}[n]=o_k[n]\gamma[n-kN] \quad (4)$$

C. Pulse Design

In the BFDM approach, the transmit pulse g is generated according to the system requirement and the received pulse γ is computed from g, as a canonical dual (bi-orthogonal). The computation methods used in this paper are as proposed in [8]. In summary, the bi-orthogonality means transmit pulse g generates a Gabor Riesz basis and equivalent dual Riesz basis is generated by receive pulse γ. As shown in [9] this can be achieved with the T^{-1} operation. While calculating the bi orthogonal pulses, side effects such as spectral re-growth due to periodic settings are negligible.

The ratio of the time and frequency pulse widths (variances) σt and σf should be almost matched to the time-frequency grid ratio.

$$\frac{T}{F}\approx\sqrt{\frac{\sigma_t}{\sigma_f}} \quad (5)$$

Pulse g is constructed based on the B-spline in the frequency domain. B-Splines were studied thoroughly in the Gabor (Weyl-Heisenberg) setting [9]. The prime reason for the usage of B-Spline pulses is due to the excellent tail properties of convolution of such pulses.

The second order B-spline (the tent) function decays faster in time and the same in frequency domain is stated as

$$B2(f)=B1(f)*B1\,(f) \quad (6)$$

Where

$$B1(f):=\chi[-1/2,1/2]\,(f) \quad (7)$$

However in practice, the transmit pulse has to be of finite duration so g(t) can be given as

$$\text{g}(t)=\left(\frac{\sin(B\pi t)}{B\pi t}\right)^2\chi(t) \quad (8)$$

III. OQAM BASED BFDM SYSTEM

In the OQAM, simultaneous transmission of real and imaginary part of a complex data symbol is not done like in QAM Scheme. The imaginary part is transmitted with a delay of half the symbol duration. The word 'offset' refers to the time shift by half the inverse of the sub-channel spacing between the real and imaginary parts of a complex symbol. For improving the peak factor, OQAM is used in single carrier systems. The difference between QAM and OQAM modulation [10] is illustrated in figure 3.

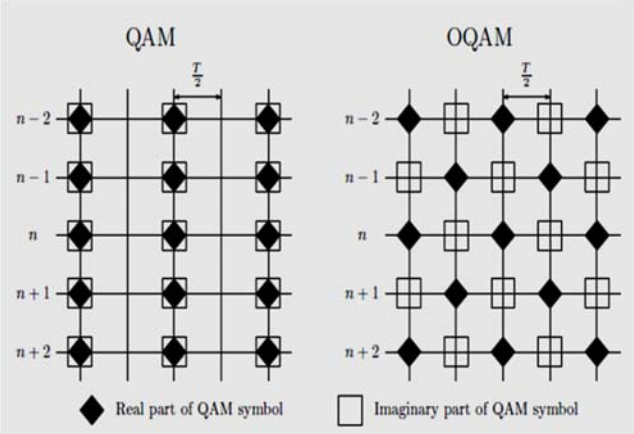

Figure 3. QAM and OQAM Symbol Transmission

OFDM/OQAM schemes are based on orthogonal modulation i.e., transmitter basis functions constitute an orthogonal basis or equivalently the transmitter filter and the receiver filter constitute a matched filter pair. However orthogonality imposes constrains on the pulse shaping filter which limit the achievable time-frequency localization. Relaxing the orthogonality requirement thereby introducing bi-orthogonal frequency division multiplexing based OQAM(BFDM-OQAM) allows to significantly improve time frequency localization of transmitter basis function which in turn yields increased dispersion robustness.

IV. SIMULATION SYSTEM SETUP

A typical wireless system can be modeled as shown in the figure 4. In the current work, BFDM transmitter, receiver and channels are modeled using MATLAB software.

The block diagram consists of :

a) *Data Source:* A random generator is used
b) *Encoding of data:* both QAM and OQAM modulator are used
c) *BFDM Modulator:* BFDM Transmitter is implemented as explained in Section II
d) *Decoding of data:* both QAM and OQAM demodulators are used
e) *BFDM Demodulator:* BFDM Receiver is implemented as explained in Section I

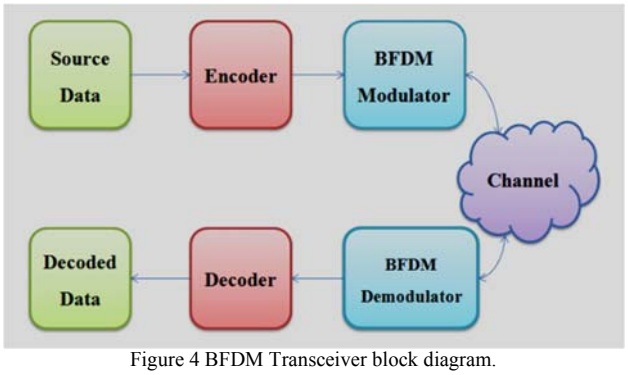

Figure 4 BFDM Transceiver block diagram.

A. Channel

In digital communication channel means a medium to send and receive the signal. In wireless channel modeling we consider Reflection, Refraction, and Scattering, these results in fading of signal. Above the large distances, the signal quality degrades even without the presence of large quantities of AWGN. Degradation is also called as fading and this is denoted as channel or fading channels. In general, fading channels Rayleigh and Rician distributions are most commonly used. In this paper, Rayleigh distribution is used, since the cellular communication is always non-Line of Sight.

B. Rayleigh distribution

Since the Line of sight (LOS) is not considered, the *Rayleigh Distribution fading represents the worst case fading conditions. As* the power is distributed quickly, the phase is evenly distributed and is independent of amplitude, mostly uses in wireless communication signal model.

C. Multipath Fading Propagation Conditions

When a signal propagates from transmitter to receiver it faces multipath. Perhaps there is Line of Sight in between a transmitter and a receiver or it can reflect to ground and then it may reach to receiver. While this reflected copy of same signal reaches to receiver they may have delay and attenuation based upon path length.

TABLE 1. EPA FADING PROFILE

Tap	Doppler frequency[HZ]	Excess tap delay[ns]	Relative Power[dB]
1	5HZ	0	0.0
2	5HZ	30	-1.0
3	5HZ	70	-2.0
4	5HZ	90	-3.0
5	5HZ	110	-8.0
6	5HZ	190	-17.2
7	5HZ	410	-20.8

There are three known LTE channel models of multipath profiles that are defined by 3GPP [11] namely: Extended Pedestrian A (EPA), Extended Vehicular A (EVA) and Extended Typical Urban (ETU) as are given in Tables 1, 2,

3. The Doppler shifts for EPA, EVA, ETU are 5Hz, 70 Hz, 300Hz respectively.

TABLE 2 EVA FADING PROFILE

Tap	Doppler frequency[HZ]	Excess tap delay[ns]	Relative Power[dB]
1	70HZ	0	0.0
2	70HZ	30	-1.5
3	70HZ	150	-1.4
4	70HZ	310	-3.6
5	70HZ	370	-0.6
6	70HZ	710	-9.1
7	70HZ	1090	-7.0
8	70HZ	1730	-12.0
9	70HZ	2510	-16.9

TABLE 3 ETU FADING MODEL

Tap	Doppler frequency[HZ]	Excess tap delay[ns]	Relative Power[dB]
1	300HZ	0	-1.0
2	300HZ	50	-1.0
3	300HZ	120	-1.0
4	300HZ	200	0.0
5	300HZ	230	0.0
6	300HZ	500	0.0
7	300HZ	1600	-3.0
8	300HZ	2300	-5.0
9	300HZ	5000	-7.0

The variation in one channel tap value from another depends on Doppler frequency, which is proportional to the mobile device speed. Higher velocity of a mobile leads to higher the Doppler frequency f_d and higher variations in the channel.

V. SIMULATION RESULTS

The BFDM system with QAM, OQAM and OFDM systems are simulated using Matlab software along with the 3GPP fading profiles and the input parameters used for the results are as shown in Table 4.

The standard carrier spacing 15 KHz of OFDM is reduced to 1.25KHz. The simulation results of the Power spectral density (PSD) for BFDM with QAM and OFDM is shown in figure 5.

From Figure 5 and 6 it can be observed that the side lobe energy suppression for BFDM systems is much better compared OFDM system. One more observation is OQAM based system has much better side lobe power suppression than QAM based system.

The simulated SER analysis for BFDM systems with QAM and OQAM and comparison with OFDM systems are presented in figure 7.

TABLE 4 INPUT PARAMETERS

Input Parameter	**Standard PRACH(OFDM)**	**Pulse shaped PRACH**
Bandwidth	1.08MHZ	1.08MHZ
Ofdm symbol duration	800μs	-
Subcarrier spacing (F)	1.25KHZ	1.25KHZ
Sampling frequency (fs)	30.72MHZ	30.72MHZ
Length of FFT (NFFT)	24576	24576
Number of subcarrier (L)	839	839
Cyclic prefix length (Tcp)	3168Ts	0
Guard time (Tg)	2976 Ts	0
Pulse length (P)	-	4ms
Number of Symbols (K)	1	1
Time-frequency product (TF)	1.25	1.25

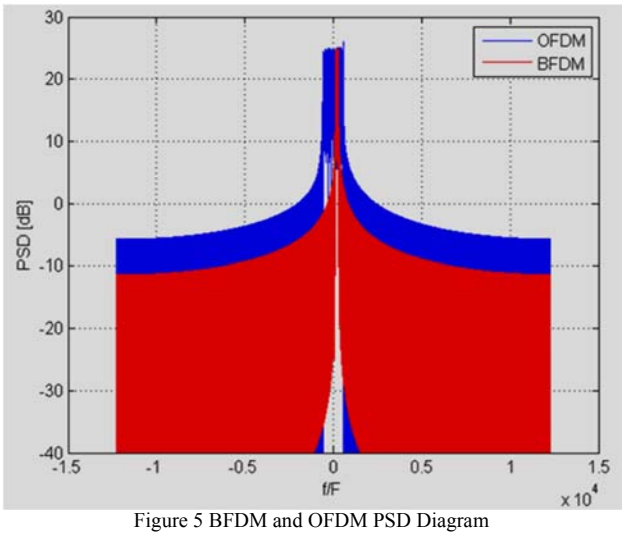

Figure 5 BFDM and OFDM PSD Diagram

The power spectral density for BFDM with OQAM and OFDM systems are as shown in figure 6

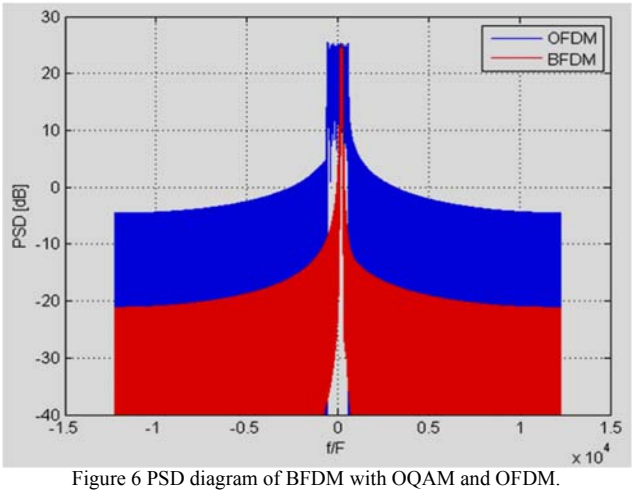

Figure 6 PSD diagram of BFDM with OQAM and OFDM.

From the figure 7 it is observed that the BFDM symbol error rate is less when compared with OFDM system under

various 3GPP defined fading profiles. As previously discussed the BFDM is more robust to frequency and time offsets and it has been proved that BFDM system performance with ETU and EVA profiles are better as the Doppler shift is higher compared to EPA profile. By observing diagrams in figure 7, one can make a note of the fact that BFDM with OQAM is performing far better than OFDM systems and slightly better compared to BFDM systems. As BFDM system is not strictly synchronized the offset errors are minimized and very much suitable for the vehicular and urban environments for Machine to Machine type communication where short messages are exchanged.

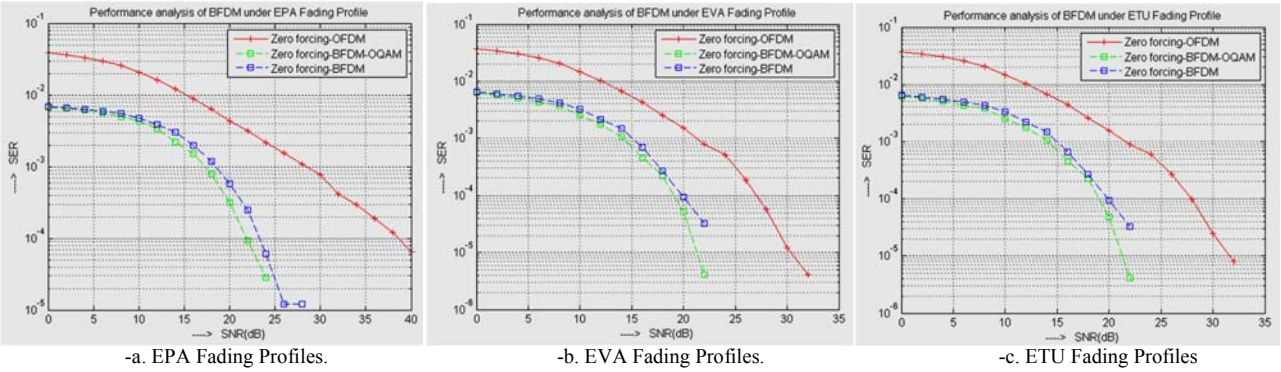

-a. EPA Fading Profiles. -b. EVA Fading Profiles. -c. ETU Fading Profiles

Figure 7 SER Performance of BFDM and OFDM systems under EPA, EVA and ETU fading profiles.

VI. CONCLUSION

In this paper, it is proven that BFDM performed well compared to OFDM under various real time fading conditions. BFDM is immune to frequency offsets that are common for cellular communications and also suitable for short message communications. The OQAM based BFDM is more immune to noise and fading and is especially well suited for IoMCT applications, where the deployments will be in urban, or highly dense areas. The side lobe suppression is very good in OQAM based BFDM system and this will lead to saving in device power which is very critical for IoMCT based applications, where hundreds of sensor devices are deployed. Since most of IoMCT applications are machine critical and are used in highly dense areas, OQAM based BFDM is most suitable candidate. The current work can be further enhanced and tested with trapezoidal pulse instead of B-Spline pulse.

REFERENCES

[1] G. Wunder, P. Jung, M. Kasparick, T. Wild, F. Schaich, Y. Chen, S. ten Brink, I. Gaspar, N. Michailow, A. Festag, L. Mendes, N. Cassiau, D. Ktenas, M. Dryjanski, S. Pietrzyk, B. Eged, P. Vago, and F. Wiedmann, "5GNOW: Non-Orthogonal, Asynchronous Waveforms for Future Mobile Applications," IEEE Communications Magazine, vol.52,no. 2, pp. 97–105, 2014.

[2] M. Kasparick, G. Wunder, P. Jung and D. Maryopi, "Bi-orthogonal Waveforms for 5G Random Access with Short Message Support," European Wireless 2014; 20th European Wireless Conference, Barcelona, Spain, 2014, pp. 1-6

[3] G. Wunder, M. Kasparick, P. Jung, "Spline Waveforms and Interference Analysis for 5G Random Access with Short Message Support",, Jan 15,2015.

[4] A. Rico-Alvarino et al., "An overview of 3GPP enhancements on machine to machine communications," in IEEE Communications Magazine, vol. 54, no. 6, pp. 14-21, June 2016.

[5] W. Kozek and A. Molisch, "Nonorthogonal pulse shapes for multicarrier communications in doubly dispersive channels," IEEE Journal Sel. Areas in Communications, vol. 16, no. 8, pp. 1579–1589, 1998.

[6] D.Schafhuber, G. Matz, and F. Hlawatsch, "Pulse-shaping OFDM/BFDM systems for time-varying channels: ISI/ICI analysis, optimal pulse design, and efficient implementation," in 13th IEEE International Symposium on Personal, Indoor and Mobile Radio Communications, vol. 3, 2002, pp. 1012–1016 vol.3.

[7] P. Jung and G. Wunder, "The WSSUS Pulse Design Problem in Multicarrier Transmission," IEEE Trans. on Communications, 2007

[8] I. Daubechies, "Ten Lectures on Wavelets," Philadelphia, PA: SIAM, 1992.

[9] V. D. Prete, "Estimates, decay properties, and computation of the dual function for Gabor frames," Journal of Fourier Analysis and Applications, 1999.

[10] Qinwei He, AnkeSchmeink, "Comparision and Evaluation between FBMC and OFDM systems",WSA 2015, March 3-5, 2015, Ilmenau, Germany.

[11] Evolved Universal Terrestrial Radio Access (E-UTRA); Base Station (BS) radio transmission and reception (3GPP TS 36.104 version 11.2.0 Release 11) (www.3GPP.org)